Creep of Zirconium and Zirconium Alloys

TROY A. HAYES and MICHAEL E. KASSNER

Cumulative zirconium and zirconium alloy creep data over a broad range of stresses (0.1 to 115 MPa) and temperatures (300 °C to 850 °C) were analyzed based on an extensive literature review and experiments. Zirconium obeys traditional power-law creep with a stress exponent of approximately 6.4 over stain rates and temperatures usually associated with the conventional ''five-power-law'' regime. The measured activation energies for creep correlated with the activation energies for zirconium self-diffusion. Thus, dislocation climb, rather than the often assumed glide mechanism, appears to be rate controlling. The common zirconium alloys (*i.e.*, Zircaloys) have higher creep strength than zirconium. The stress exponents of the creep data in the five-power-law regime were determined to be 4.8 and 5.0 for Zircaloy-2 and Zircaloy-4, respectively. The creep strength of irradiated Zircaloy appears to increase relative to unirradiated material. It was found that the creep behavior of zirconium was not sensitive to oxygen in the environment over the temperature range examined.

I. INTRODUCTION

CREEP of zirconium and zirconium alloys has often been described as ''anomalous.'' Researchers often report that zirconium and zirconium alloys never reach true steady-state creep (*e.g.*, References 1 through 3). It has also been reported that the stress exponent[4,5,6] and activation energy[4–7] change continuously with stress, not reflective of climb control as most other ''pure'' metals within the ''five-power-law'' regime. Many interpretations have been offered explaining the creep behavior of zirconium. Some have suggested that creep is dislocation-climb-controlled in the ''intermediate-stress'' regime corresponding to the five-power-law regime,[7–10] as in other metals and alloys, while others maintain that creep is dislocation-glide-controlled.[4,6] Still others suggest several different controlling mechanisms within the five-power-law regime depending on stress and temperature.[5,11] The creep rate of zirconium at stresses below those associated with five-power-law creep has been reported to vary nearly linearly with stress. The details of low-stress creep behavior of zirconium are discussed in detail elsewhere.[12] A limited amount of low-stress creep data for Zircaloy-2 suggests that the stress exponent, n, of the steady-state creep rate is approximately equal to one in this regime ($n \equiv d \log \dot{\varepsilon}_{ss} / d \log \sigma_{ss}$, where $\dot{\varepsilon}_{ss}$ is the steady-state creep rate and σ_{ss} is the steady-state creep stress). Recent analysis by Blum and Maier on aluminum, however, suggests that steady-state conditions may not be achieved in this regime and that the true stress exponent, n, may not approach one.[13] Aluminum obeys classic creep behavior and similar arguments may also apply to other pure metals and class M alloys (such as Zircaloys).

Conclusions about zirconium and zirconium alloy creep behavior in the intermediate stress regime often reflect the analysis of limited data. Cumulative zirconium and zirconium alloy creep data will be presented here based on an extensive literature review that includes data often not included in earlier analyses and on experimental results for zirconium and Zircaloy-2 creep from the current study.

TROY A. HAYES, Managing Engineer, is with Exponent Failure Analysis Associates, Menlo Park, CA 94025. MICHAEL E. KASSNER, Department Chair, is with the Aerospace and Mechanical Engineering Department, University of Southern California, Los Angeles, CA 90089.

Manuscript submitted September 19, 2005.

It has been shown that oxygen absorption has detrimental effects on the creep strength of titanium,[14,15] which shares many common properties with zirconium. Raff and Meyder[16] suggest that the creep strength of Zircaloy in an oxidizing atmosphere is higher than that of Zircaloy in an inert atmosphere at temperatures greater than 1000 °C, but that the opposite is true at temperatures between 600 °C and 1000 °C as a result of oxide cracking. Raff and Meyder did not discuss the effects of oxidation on the creep strength below 600 °C. The effect of atmosphere on the creep properties of zirconium was evaluated in this study by conducting creep tests on uncoated zirconium in air, uncoated zirconium in argon, and platinum-coated zirconium in air.*

*Platinum has been shown to be an effective oxygen barrier during creep of titanium.[14]

One common application of zirconium alloys is as nuclear fuel cladding in nuclear fission reactors. The zirconium alloy cladding is relied upon to contain the fuel safely long after removal from the reactor. Lifetime creep modeling requires knowledge of the behavior of irradiated zirconium alloys. The effects of irradiation on the creep properties of zirconium alloys will be discussed in this article.

II. EXPERIMENTAL PROCEDURE

The zirconium used in this study was obtained in the form of a 19.7-mm nominal-diameter rod from Allegheny Wah Chang (Albany, OR). The processing consisted of several heating (at temperatures ranging from 704 °C to 772 °C), forging, sand blasting, and pickling (acid etching) steps until the final diameter was achieved. The chemical composition is listed in Table I.

The Zircaloy-2 used in this study was obtained in the form of a 16-mm-diameter rod from Allegheny Wah Chang. The processing consisted of several heating (at temperatures ranging from 660 °C to 1110 °C), forging, sand blasting, and pickling (acid etching) steps until the final diameter was achieved. The chemical composition is listed in Table II.

Table I. Compsition of the Zirconium Used in This Study; Zirconium Reported in Weight Percents and All Others in Parts per Million (as Reported by Allegheny Wah Chang)

Element (ppm)				
Al <20	B < 0.25	C 25	Ca <10	Cd < 0.25
Cl < 5	Co <10	Cr <50	Cu <25	Fe 150
H < 3	Hf <46	Mg <10	Mn <25	Mo < 10
N <20	Na < 5	Nb <50	Ni <35	O 420
P < 3	Pb <25	Si <10	Sn <10	Ta < 50
Ti <25	U < 1	V <25	W <25	Zr 99.9 pct

Table II. Composition of the Zircaloy-2 Used in This Study: Elements in the First Column are Reported in Weight Percents and All Other Elements are Measured in Parts per Million (as Reported by Allegheny Wah Chang)

Element (Wt Pct)	Element (ppm)		
Zr 98.25	Al 29	H < 3	Nb <50
Cr 0.10	B 0.3	Hf 52	Pb <25
Fe 0.19	C 133	Mg <10	Si 91
Ni 0.07	Cd < 0.2	Mn <25	Ti 29
O 0.13	Co < 10	Mo <10	U < 1
Sn 1.26	Cu < 25	N 32	W <50

Cylindrical tensile specimens were machined from the as-received zirconium and Zircaloy-2 rod. The tensile specimens were subsequently annealed at the Albany Research Center in evacuated quartz tubes for half an hour at 780 °C, in a vacuum of 10^{-1} to 10^{-2} Pa. The average grain size of the annealed zirconium was determined to be 58 μm using the average line-intercept method, and was consistent in both the transverse and longitudinal (axial) directions. The average grain size of the annealed Zircaloy-2 was 7 μm in the transverse direction and 8 μm in the longitudinal direction.

As mentioned previously, one objective of this study was to establish the importance of testing atmosphere on the creep properties of zirconium. The effect of atmosphere on the creep properties of zirconium was evaluated by conducting creep tests on uncoated zirconium in air, uncoated zirconium in argon, and platinum-coated* zirconium in air. Platinum was chosen as a coating because of its inert properties and because it has been shown to be an effective oxygen barrier during creep of titanium.[17]

*The samples were sputter coated with Pt to a thickness 1.2 μm by Implant Sciences Corporation (Wakefield, MA).

Constant true-stress uniaxial creep tests were performed on the uncoated and Pt-coated zirconium specimens between 8 and 70 MPa and 350 °C to 700 °C in air. Constant true-stress uniaxial creep tests were performed on the Zircaloy-2 specimens between 24 and 52 MPa and 500 °C and 600 °C in air. The creep tests were performed on a Satec dead weight creep-testing machine with a three-zone furnace, which maintained a constant temperature profile along the length of the specimen to within 1 °C. Strain was measured *in situ* using a high-temperature Measuretron Series 4112 linear variable displacement transducer extensometer with an accuracy of approximately 0.02 pct. Constant stress was maintained in all tests by incrementally removing weights from the load after every 1 to 2 pct strain. The uncoated creep samples were wrapped in titanium foil to help mitigate oxygen absorption. Two additional constant true-stress uniaxial creep tests were performed on cylindrical uncoated zirconium specimens in argon on an Instron (Norwood, MA) 8521 servo-hydraulic tensile testing machine with collet-type grips and an ATS (Applied Testing Systems, Inc., Butler, PA) 3-zone furnace. These samples were wrapped with titanium foil to further protect against oxygen absorption.

Two constant strain-rate creep tests were performed in air on uncoated cylindrical Zircaloy-2 specimens at a strain rate of 5×10^{-5} s^{-1} and temperatures of 300 °C and 350 °C to evaluate the creep fracture behavior of Zircaloy-2.

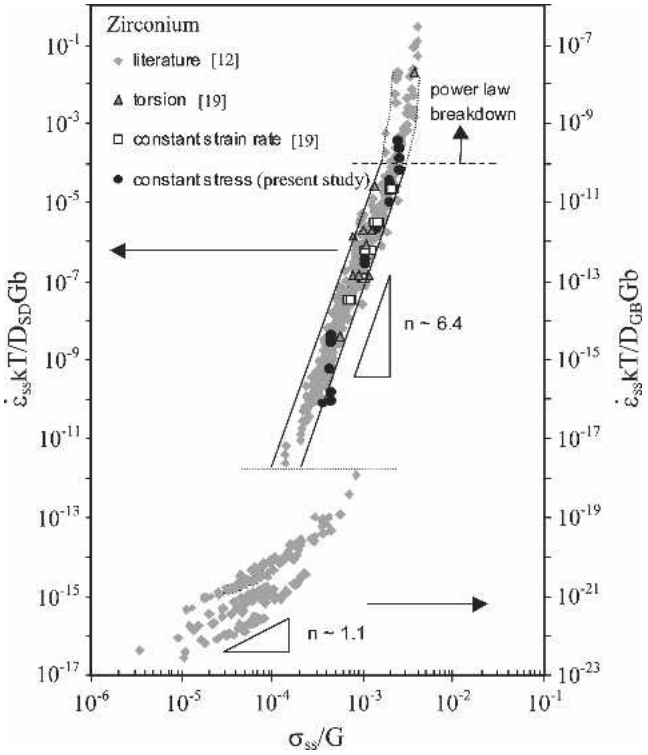

Fig. 1—Diffusion coefficient-compensated steady-state strain rate *vs* modulus-compensated steady-state stress data for zirconium from the literature (99.8 to 99.95 pct Zr),[12] the current study, and Perez-Prado *et al.*[19] (99.8 pct Zr).

III. RESULTS AND DISCUSSION

A. *Creep Behavior of Zirconium*

In the past, a variety of explanations have been presented to describe the creep behavior of zirconium and zirconium alloys over a range of stresses and temperatures. These analyses (*e.g.*, References 4 through 6) suggest several different controlling mechanisms depending on the temperature and stress. These interpretations were often developed to explain the creep behavior observed in individual creep studies. However, when comprehensive data are analyzed, more reliable, and often different, interpretations emerge.

Zirconium creep data from various studies are presented in Figure 1, which is a plot of the diffusion coefficient

compensated steady-state strain (creep) rate* *vs* the modulus-compensated steady-state creep stress (σ_{ss}). Data in the moderate σ/G (five-power-law) and high σ/G (power-law breakdown) regimes are normalized by a diffusion coefficient with an activation energy, Q, of 270 kJ/mol and a (typical) pre-exponential, D_o, of 5×10^{-4} m^2/s.[12] Data in the low σ/G regime are normalized by a diffusion coefficient with an activation energy of 90 kJ/mol and a pre-exponential of 5×10^{-4} m^2/s.[12]

*Some data in Figure 1 represent minimum strain rates rather than steady-state strain rates, but it was determined that the strain rates in these tests were close to the steady-state strain rate.

It is apparent from Figure 1 that a cumulative plot developed from all zirconium creep data appears to be consistent with typical creep behavior for class II (M) metals and alloys.[18] At low σ/G, the data in Figure 1 have a constant slope (stress exponent, n) of approximately 1.1, perhaps indicative of Harper–Dorn or diffusional creep. At intermediate values of σ/G, the data have a constant stress exponent of approximately 6.4, which is within the range of so-called five-power-law creep. Zirconium reaches power-law breakdown at values of compensated stress above approximately 2×10^{-3}, where the stress exponent then increases with increasing σ/G.

In the intermediate stress regime, there is an established, largely phenomenological, relationship between the steady-state strain rate, $\dot{\varepsilon}_{ss}$ (or creep rate), and stress, σ_{ss}, for steady-state five-power-law creep in pure metals and class II (or M) alloys:

$$\dot{\varepsilon}_{ss} = A_0 \exp\left[\frac{-Q_{SD}}{kT}\right]\left(\frac{\sigma_{ss}}{G}\right)^n \qquad [1]$$

where A_0 is a constant; k is Boltzmann's constant; Q_{SD} is the self-diffusion activation energy; G is the shear modulus; and n is the stress exponent, which varies from approximately 4 to 7.[18] The zirconium data in the moderate σ/G regime of Figure 1 indicate a constant stress exponent of approximately 6.4, typical of five-power-law creep.

Well-defined subgrain boundaries, classically, readily form during early primary creep over the five-power-law regime.[18] Conversely, these subgrains form sluggishly, if formed at all, only well into steady-state creep during viscous-glide-controlled creep.[18,20] Recent transmission electron microscopy on creep-deformed zirconium indicates that subgrains do form during steady-state creep of zirconium,[19] further supporting dislocation-climb-controlled creep.

The creep activation energy is compared to the self-diffusion activation energy in Figure 2, which is based on the data presented in References 12, 19, and 21–27.[21–27] A discussion of the change in self-diffusion activation energy as a function of temperature is discussed in detail elsewhere.[12] Briefly, it has been suggested that the reason for the change in self-diffusion activation energy is due to the effect of iron on the self-diffusion of zirconium (*e.g.*, Reference 28). The diffusion coefficient of (interstitial) iron in zirconium has been reported to be approximately eight orders of magnitude faster than the zirconium self-diffusion coefficient over a range of temperatures.[28] The activation energy for lattice self-diffusion appears to decrease at higher temperatures due to Fe-vacancy interaction. Iron is believed to interact strongly with vacancies[21] and, possibly, form Fe-vacancy pairs.[28,29,30] Interstitial diffusion of Fe-vacancy pairs may increase zirconium self-diffusion and decrease the high-temperature self-diffusion activation energy. The increase in self-diffusion activation energy at lower temperatures to values closer to that of the ''intrinsic'' self-diffusion coefficient was suggested to occur because of a decrease in Fe solubility at these temperatures. Activation energies calculated from the constant-stress creep data in the current study and the data from Reference 19 are consistent with the general creep activation energy trends observed in the literature (Figure 2). Specifically, the creep activation energy appears to increase with increasing temperature from around 170 kJ/mol at 375 °C to approximately 300 to 350 kJ/mol around 600 °C. The activation energy for creep then drops to approximately 100 kJ/mol at temperatures above 650 °C. The self-diffusion activation energy for zirconium behaves similarly, decreasing from around 270 kJ/mol to 650 °C to approximately 100 to 200 kJ/mol at temperatures of 650 °C to 850 °C. Although there is a fair amount of scatter in both the creep and self-diffusion activation energies, the general consistency between them supports dislocation-climb-controlled (self-diffusion-controlled) creep in the five-power-law regime.

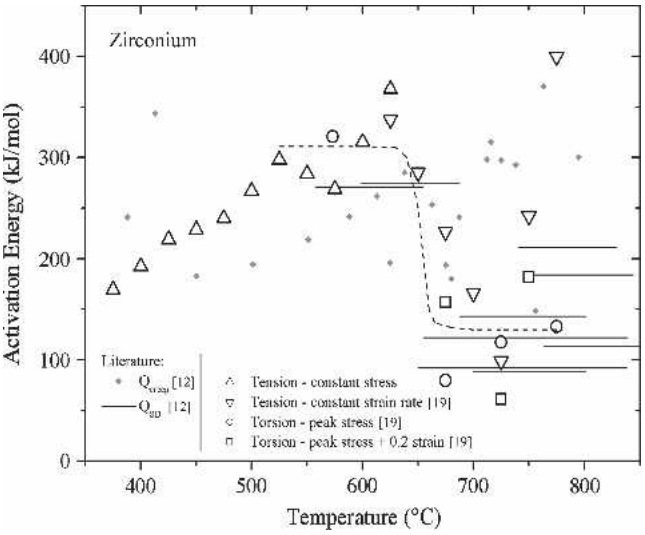

Fig. 2—Creep (points) and self-diffusion activation energies (lines) as a function of temperature. All measurements from the literature are based on 99.95 or 99.8 pct pure Zr. The impurities may affect the activation energy. The creep activation energies were calculated based on data in References 4, 5, and 7. The self-diffusion activation energies were taken from References 21 through 27. The constant stress data (△) are from the current study, while the constant strain rate tension (▽) and torsion data (○, □) are from Reference 19.

B. *Effects of Atmosphere*

Zirconium creep tests were performed under three different atmospheric conditions (in air, in argon, and Pt coated in air). These three conditions were chosen in order to determine whether oxygen absorption or oxidation had a significant effect on the zirconium creep properties. Representative creep curves from this study are shown in Figure 3. All creep curves can be found in Reference 31. The data

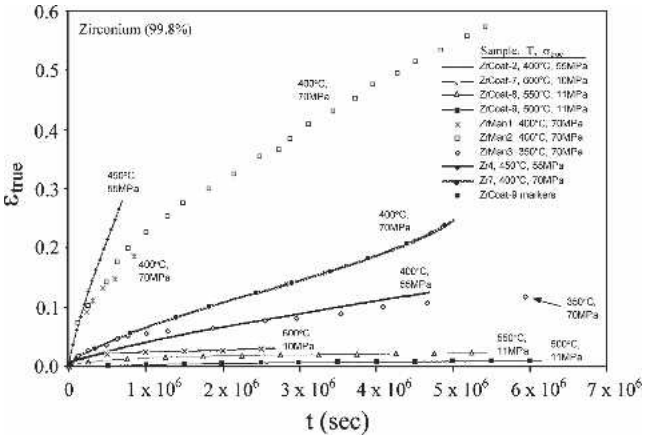

Fig. 3—Representative zirconium creep curves tested in air. ZrCoatX indicate Pt-coated specimens, while the other specimens were uncoated.

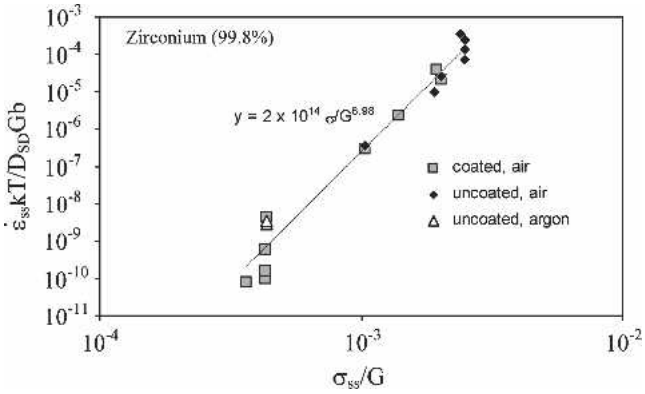

Fig. 4—Comparison of creep results from tests of uncoated zirconium in air, uncoated zirconium in argon, and Pt-coated zirconium in air.

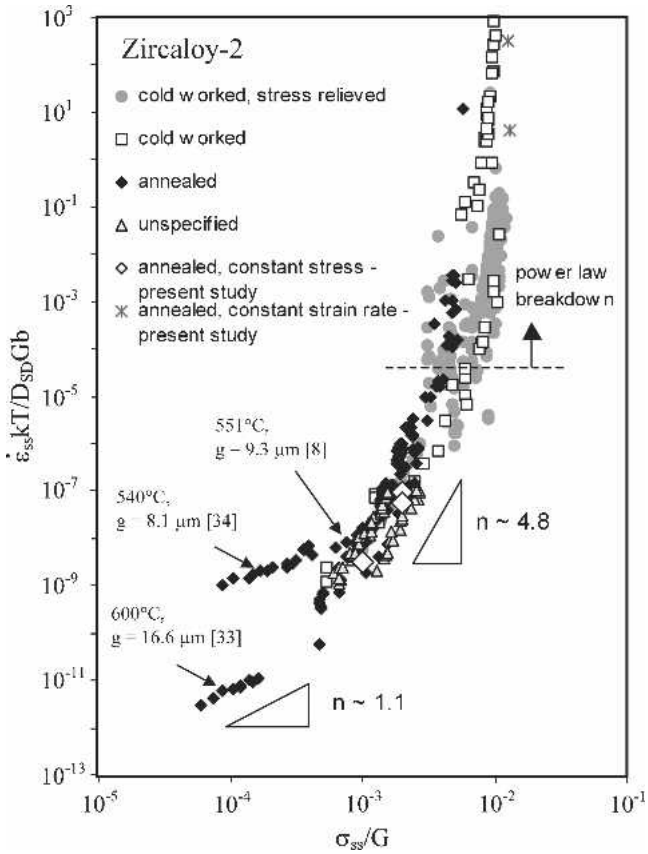

Fig. 5—Diffusion-coefficient-compensated steady-state strain rate *vs* modulus-compensated steady-state stress data for Zircaloy-2 from Jones,[33] Wood,[35] Rose and Hindle,[36] Ross-Ross and Hunt,[37] Clay and Redding,[38,39] Bernstein,[8] Prasad *et al.*,[40,41] Fidleris,[2,3] Coleman,[42] Burton *et al.*,[43] Lucas *et al.*,[44,45,46] Pankaskie,[47] Bell,[48] Tinti,[49] Gilbert and Mastel,[50] and the current study.

from all zirconium creep tests are presented in Figure 4. Although there is a fair amount of scatter among the data for reasons that are unclear, it is apparent in Figure 4 that the creep rate was not very sensitive to the testing atmosphere over the range of conditions tested.

C. *Effects of Alloying*

Data from various studies on the creep of Zircaloy-2* and Zircaloy-4** are shown in Figures 5 and 6, respectively, which are plots of the diffusion-coefficient-compensated steady-state strain (creep) rate *vs* the modulus-compensated steady-state creep stress. Some of the creep data in both figures represent the reported minimum creep rate rather than the steady-state creep rate (it was not clear whether steady state had been achieved in those tests). The modulus-compensated effective (von Mises) stress is plotted for non-uniaxial creep data. Data in Figures 5 and 6 are normalized by a diffusion coefficient with an activation energy, Q, of 270 kJ/mol and a (typical) pre-exponential, D_o, of 5×10^{-4} m^2/s, consistent with the value used for zirconium. This activation energy is close to the (constant) creep activation energy of 245 kJ/mol measured by Holmes for Zircaloy-2 between approximately 250 °C and 500 °C.[32]

Zircaloy-2 (Figure 5) and Zircaloy-4 (Figure 6) exhibit typical five-power-law creep behavior, similar to the behavior of zirconium. Zircaloy-2 exhibits one-power-law creep for values of σ/G below approximately 10^{-3}, five-power-law creep for values of σ/G between approximately 10^{-3} and 5×10^{-3}, and power-law breakdown for values of σ/G above approximately 5×10^{-3}. The average slope (power-law exponent, n) of the Zircaloy-2 data in the five-power-law regime was determined to be approximately 4.8. Although no creep data for Zircaloy-4 in the one-power-law regime were found, it appears that Zircaloy-4 exhibits five-power-law creep for values of σ/G below approximately 5×10^{-3} and exhibits power-law breakdown for larger modulus-compensated stresses. The average slope (power-law exponent, n) of the Zircaloy-4 data in the five-power-law regime was determined to be approximately 5.0.

The creep behaviors of Zircaloy-2 and Zircaloy-4 are compared with the behavior of zirconium in Figure 7,

*Zircaloy-2 has an alloying-element composition of approximately 1.5 pct Sn, 0.15 pct Fe, 0.10 pct Cr, and 0.05 pct Ni.

**Zircaloy-4 has an alloying-element composition of approximately 1.5 pct Sn, 0.20 pct Fe, and 0.10 pct Cr.

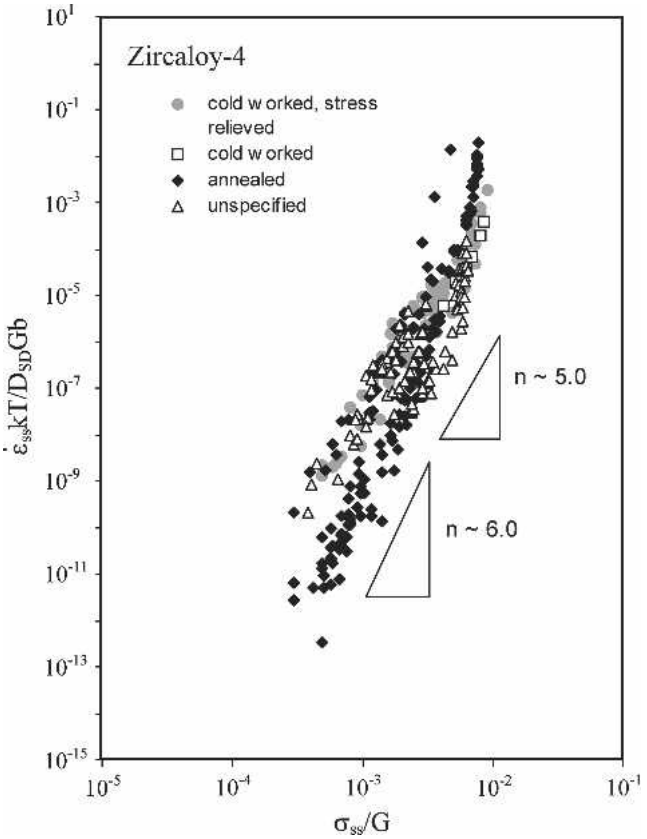

Fig. 6—Diffusion-coefficient-compensated steady-state strain rate *vs* modulus-compensated steady-state stress data for Zircaloy-4 from Matsuo,[51] Povolo and Marzocca,[52] Donaldson and Ecob,[1,53] Busby *et al.*,[54,55] Garde *et al.*,[56,57,58] Brun *et al.*,[59] Mayuzumi and Onchi,[60,61] Murty *et al.*,[62,63,64] Kim,[65] Choe and Hong,[66] Park *et al.*,[67] and Rosinger *et al.*[68]

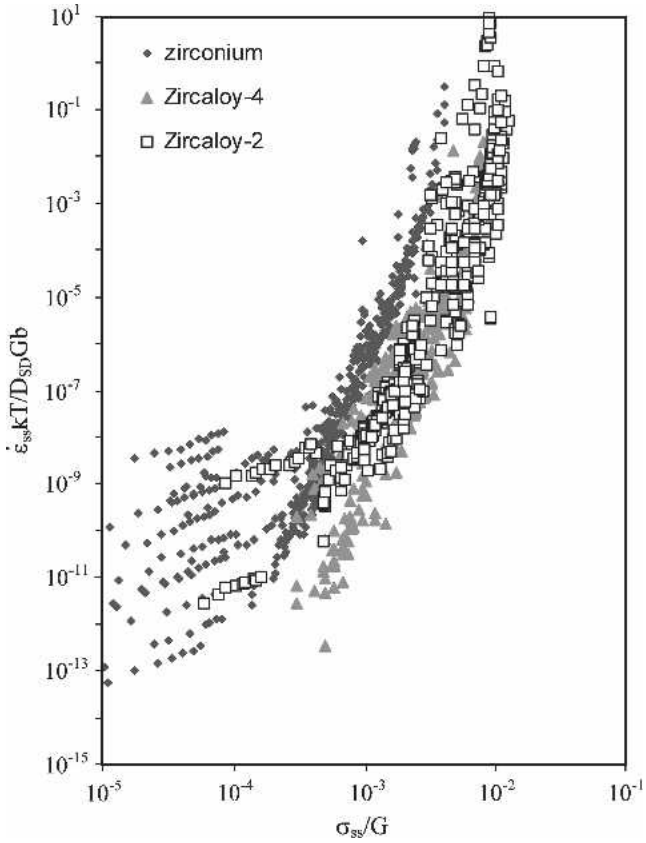

Fig. 7—Diffusion-coefficient-compensated steady-state strain rate *vs* modulus-compensated steady-state stress for zirconium, Zircaloy-2, and Zircaloy-4 (refer to Figures 1, 5, and 6 for references).

which is a plot of all the creep data presented in Figures 1, 5, and 6. It is apparent in Figure 7 that the addition of alloying elements increases the creep strength of zirconium and that the creep behavior of both Zircaloy-2 and Zircaloy-4 are quite similar. The only notable difference between the creep behavior of Zircaloy-2 and Zircaloy-4 occurs at values of compensated strain rate below approximately 10^{-9}, where it appears that Zircaloy-4 has higher creep strength than Zircaloy-2. The Zircaloy-2 data in this region appear to obey one-power-law creep, while the Zircaloy-4 data maintain the five-power-law relationship. The cause of this difference is unclear. Another characteristic that is apparent in Figure 7 is that the scatter among the Zircaloy-2 and Zircaloy-4 data are much greater than is seen in the zirconium data. This is due, in large part, to several factors that will be discussed subsequently.

First, it was noted that the composition varies significantly between various batches or manufacturers of Zircaloy-2 and Zircaloy-4, such that there is a certain amount of variation between the percentage of alloying elements in any given set of Zircaloy creep specimens tested in the various studies that were used to develop Figure 7. This variation in the composition is inherent because the composition limits for Zircaloy-2 and Zircaloy-4 are defined as a range. For zirconium, however, almost all the prior investigations reviewed in this study used commercially pure zirconium with a nominal composition of approximately 99.8 pct Zr.

Second, the zirconium creep data in the literature almost exclusively used uniaxial creep tests. Creep data reported for Zircaloy-2 and Zircaloy-4 include uniaxial creep data, hoop creep data for internally pressurized tubes, biaxial creep tests of flat plate, and several other test configurations. (The modulus-compensated effective (von Mises) stress was used when plotting data from nonuniaxial creep tests.)

Third, the creep data reported for Zircaloy-2 and Zircaloy-4 included materials with varying thermomechanical histories. Some tests used cold-worked (CW) material, others used material that was cold worked and stress relieved (CWSR), while others used material that was partially or fully annealed. The creep data in Figures 5 and 6 were divided into four processing histories: CW, CWSR, annealed, and unspecified. As can be seen in Figure 5 (Zircaloy-2), the data measured for all four processing histories appear to obey similar trends. The creep strength of the CW and CWSR Zircaloy-2, however, appears higher than the creep strength of the fully annealed Zircaloy-2 at high compensated stresses. Similar to Zircaloy-2, the creep strength of the CW and CWSR Zircaloy-4 (Figure 6) appears higher than the creep strength of the fully annealed Zircaloy-4 at high compensated stresses. Curiously, the stress exponent of fully annealed Zircaloy-4 appears to be

higher than the stress exponent of CWSR Zircaloy-4 in the intermediate stress regime and the creep strength of the annealed material is higher than the CWSR material in this regime. It is unclear why the creep strength of the annealed material would be higher than that of the CWSR material in this regime, unless, perhaps, recrystallization occurred early in the creep studies on the CWSR material, reducing the creep strength below that of a fully annealed material that had not undergone the same level of cold work. The stress exponent of 6.0 that was measured for the CWSR Zircaloy-4 is very close to the value of 6.4 observed for zirconium (Figure 1). No low stress data for Zircaloy-4 were reported in the literature.

D. *Effects of Irradiation*

All the creep data discussed to this point were measured on unirradiated zirconium and zirconium alloys. Zirconium alloys are commonly used as cladding for nuclear fuel in nuclear fission reactors. After removal from reactor, the fuel rods (spent nuclear fuel, or ''SNF'') are often stored in stainless steel-lined concrete casks for extended periods of time. During dry storage, the zirconium alloy cladding is subjected to elevated temperatures and stresses. It is important to establish the creep properties of irradiated zirconium alloys so that the long-term behavior and safety of the spent nuclear fuel can be verified. It has generally been accepted that the creep of irradiated Zircaloys can be conservatively modeled by using the creep characteristics of unirradiated Zircaloy because using such modeling should overpredict the creep rate and total creep strain. Porsch *et al.* reported that the level of creep strain observed during post-dry storage creep tests on (irradiated) SNF was lower than the level predicted based on unirradiated creep data.[69] Peehs and Fleisch reported similar results based on creep tests of (irradiated) SNF, where they noted ''markedly reduced'' creep rates in the irradiated material compared to unirradiated creep data.[70] Kaspar *et al.* reported creep rates during testing of (irradiated) SNF that were approximately half the creep rates predicted based on unirradiated creep data.[34] No actual creep data were reported in these studies so an independent comparison to unirradiated creep data was not possible. Postdry storage (irradiated) creep data for Zircaloy-4 from Einziger *et al.*[71,72,73] and Goll *et al.*[74] are compared to the unirradiated creep data in Figure 8. The irradiated data from Einziger *et al.,* measured in 2003,[69] represent steady-state creep data, while the rest of the irradiated data represent average creep rates calculated from the data reported in the respective studies. The average creep rate was calculated by taking the total observed creep strain divided by the total test time.

It is apparent in Figure 8 that the creep behavior of irradiated Zircaloy-4 is quite similar to that of unirradiated Zircaloy-4, at least for the conditions used in the tests of irradiated Zircaloy-4 shown here, except the data by Goll *et al.*,[74] which indicated significantly higher creep strength in the irradiated material. All the other irradiated data plotted in Figure 8 appear to fit well within the range of unirradiated creep data. It should be noted, however, that the creep rates of the ''average'' irradiated creep data shown in Figure 8 are overestimated because the average creep rate was calculated by simply dividing the total creep strain by the total creep-test duration. The steady-state creep rate, however, is the minimum creep rate that would be observed over an entire test (assuming steady-state conditions are achieved). The average creep rates are based on total strains that are a composite of primary, secondary (possibly), and even tertiary (possibly) creep strain. The average creep rates overestimate the steady-state creep rate because the primary and tertiary creep rates are much higher than the steady-state creep rate. The steady-state creep rates in Figure 8 for these data would therefore be shifted ''down'' to lower strain rates. These data, which currently appear to fall in the middle of the range of unirradiated creep data, would then indicate higher creep strength than the average unirradiated data. Thus, it appears that irradiation increases the creep strength of Zircaloys based on the available creep data. The effect that irradiation has on the transition stress between the one-power-law and five-power-law regimes is unclear because no low stress-irradiated creep data were reported.

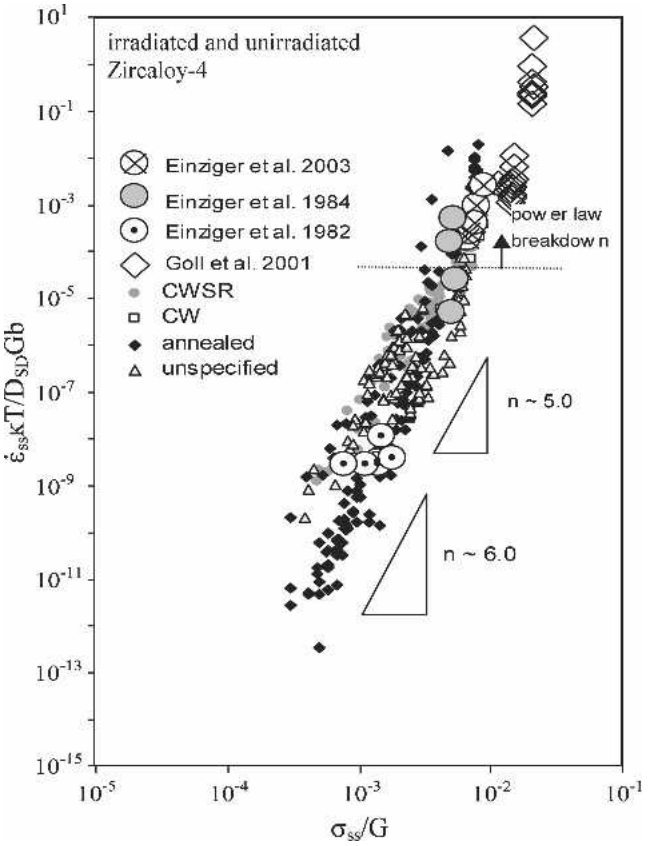

Fig. 8—Comparison of the diffusion-coefficient-compensated steady-state strain rate *vs* modulus-compensated steady-state stress data for irradiated and unirradiated Zircaloy-4. References for the unirradiated data can be found in (Figure 6). The irradiated creep data are from Einziger *et al.*[71,72,73] and Goll *et al.*[74]

E. *Creep Fracture*

It has been suggested that zirconium alloys are resistant to void formation and that creep cavitation plays little or no role in the creep failure of these alloys,[75,76] contrary to the results of a study by Keusseyan *et al.*[77] In order to

investigate the failure mechanism of zirconium alloys, two cylindrical Zircaloy-2 specimens were tested to failure under constant strain-rate conditions. The details of the creep fracture tests and results are described elsewhere.[78] Briefly, SEM examinations of the fracture surfaces and cross sections of the material near the fracture surfaces revealed extensive cavitation damage. These results, combined with an examination of the initial material condition and condition during steady-state creep, suggest that failure of Zircaloy under conditions relevant to the dry storage of spent nuclear fuel occurs by a cavity nucleation, growth, and interlinkage mechanism.

IV. CONCLUSIONS

Zirconium obeys traditional power-law creep with a stress exponent of approximately 6.4 over stain rates and temperatures usually associated with the conventional five-power-law regime. The creep activation energies also correlated with the self-diffusion activation energies. Thus, dislocation climb, rather than the often assumed glide mechanism, is likely rate controlling. The creep behavior of zirconium was not sensitive to oxygen in the environment over the temperature range examined. Alloying zirconium increases the creep strength over all creep regimes. The slope (stress exponent) of the creep data in the five-power-law regime was determined to be 4.8 and 5.0 for Zircaloy-2 and Zircaloy-4, respectively. Irradiation appears to increase the creep strength of zirconium alloys.

ACKNOWLEDGMENTS

This work was performed under the auspices of the United States Department of Energy (DOE) by Lawrence Livermore National Laboratory (LLNL) under Contract No. W-7405-ENG-48, and a subcontract from LLNL to the University of California, San Diego, under Contract No. B345708 515. The financial support from the DOE National Spent Nuclear Fuel Program and Office of Spent Fuel Management (EM-67), the Materials Research Institute at Lawrence Livermore National Laboratory, and Sigma Xi is greatly appreciated.

REFERENCES

1. R.C. Ecob and A.T. Donaldson: *J. Nucl. Mater.*, 1985, vol. 132, pp. 110-25.
2. V. Fidleris: *J. Nucl. Mater.*, 1968, vol. 26, pp. 51-76.
3. V. Fidleris and C.D. Williams: *Electrochem. Technol.*, 1966, vol. 4, pp. 258-67.
4. A.J. Ardell and O.D. Sherby: *Trans. TMS-AIME*, 1967, vol. 239, pp. 1547-56.
5. E.R. Gilbert, S.A. Duran, and A.L. Bement: *Applications-Related Phenomena for Zirconium and Its Alloys*, ASTM STP 458, ASTM, Philadelphia, PA, 1968, pp. 210-25.
6. S.R. MacEwen, R.G. Fleck, E.T.C. Ho, and O.T. Woo: *Metall. Trans. A*, 1981, vol. 12A, pp. 1751-59.
7. M. Pahutova and J. Cadek: *Mater. Sci. Eng.*, 1973, vol. 11, pp. 151-62.
8. I.M. Bernstein: *Trans. TMS-AIME*, 1967, vol. 239, pp. 1518-22.
9. B. Ramaswami and G.B. Craig: *Trans. TMS-AIME*, 1967, vol. 239, pp. 1226-31.
10. N. Prasad, G. Malakondaiah, and P. Rama Rao: *Trans. Ind. Inst. Met.*, 1989, vol. 42 (supplement), pp. S165-74.
11. H. Siethoff and K. Ahlborn: *Scripta Metall.*, 1987, vol. 21A, pp. 1439-44.
12. T.A. Hayes, M.E. Kassner, and R.S. Rosen: *Metall. Mater. Trans. A*, 2002, vol. 33A, pp. 337-43.
13. W. Blum and W. Maier: *Phys. Status Solidi*, 1999, vol. 171, pp. 467-74.
14. S. Fujishiro and D. Eylon: *Scripta Metall.*, 1977, vol. 11, pp. 1011-16.
15. C. Quesne, C. Duong, F. Charpentier, J. Fries, and P. Lacombe: *J. Less-Common Met.*, 1979, vol. 68, pp. 133-42.
16. S. Raff and R. Meyder: *Water Reactor Fuel Element Performance Computer Modeling*, Applied Science Publishers, London, 1983, p. 253.
17. S. Fujishiro and D. Eylon: *Scripta Metall.*, 1977, vol. 11, pp. 1011-16.
18. M.E. Kassner and M.-T. Perez-Prado: *Fundamentals of Creep in Metals and Alloys*, Elsevier, Oxford, 2006.
19. M.T. Pérez-Prado, S.R. Barrabes, M.E. Kassner, and E. Evangelista: *Acta Mater.*, 2005, vol. 53, pp. 581-91.
20. G.A. Henshall, M.E. Kassner, and H.J. McQueen: *Metall. Mater. Trans. A*, 1992, vol. A23, pp. 881-89.
21. M. Lubbehusen, K. Vieregge, G.M. Hood, H. Mehrer, and C. Herzig: *J. Nucl. Mater.*, 1991, vol. 182, pp. 164-69.
22. J. Horvath, F. Dyment, and H. Mehrer: *J. Nucl. Mater.*, 1984, vol. 126, pp. 206-14.
23. F. Dyment and C.M. Libanati: *J. Mater. Sci.*, 1968, vol. 3, pp. 349-59.
24. G.B. Fedorov and F.I. Zhomov: *Met. Metalloved. Chistyh. Metall.*, 1959, vol. 1, p. 161.
25. E.V. Borisov, Yu. G. Godin, P.L. Gruzin, A.J. Evstyukhin, and V.S. Emel'yanov: *Metall. Metallogr.*, 1958, p. 291.
26. V.S. Lyashenko, V.N. Bykov, and L.V. Pavlinov: *Phys. Metall. Metallogr.*, 1959, vol. 8, pp. 40-46.
27. P. Flubacher: "Selbst-Diffusionsversuche in α-Zirkon," EIR-Bericht No. 49, Eidg. Institut für Reaktorforschung, Würenlingen, Switzerland, 1963.
28. G.M. Hood: *Defect Diff. Forum*, 1993, vols. 95–98, pp. 755-74.
29. W. Frank: *Defect Diff. Forum,* 1989, vols. 66–69, pp. 387-94.
30. E. Forlerer de Svarch and C. Rodriguez: *J. Nucl. Mater.*, 1991, vol. 185, pp. 167-73.
31. T.A. Hayes: Ph.D. Dissertation, University of California, San Diego, CA, 2004.
32. J.J. Holmes: *J. Nucl. Mater.*, 1964, vol. 13, pp. 137-41.
33. R.B. Jones: *J. Nucl. Mater.*, 1966, vol. 19, pp. 204-07.
34. G. Kaspar, M. Peehs, E. Steinberg, and H. Schonfeld: *Trans. 8th Int'L SMiRT Conf.*, North Holland, Amsterdam paper C1/8, 1985, pp. 51-7.
35. D.S. Wood and B. Watkins: *J. Nucl. Mater.*, 1971, vol. 41, pp. 327-40.
36. K.M. Rose and E.D. Hindle: *Zirconium in the Nuclear Industry*, ASTM STP 633, ASTM, Philadelphia, PA, 1977, p. 24.
37. P.A. Ross-Ross and C.E.L. Hunt: *J. Nucl. Mater.*, 1968, vol. 26, pp. 2-17.
38. B.D. Clay and G.B. Redding: "Creep Rupture Properties of Alpha-Phase Zircaloy Cladding Relevant to the Loss-of-Coolant Accident," CEGB Report No. RD/B/N 3187, 1975, Berkeley Nuclear Laboratories Report No. CEGB-RD/B/N 3782, Berkeley, England, 1976.
39. B.D. Clay and G.B. Redding: *J. Br. Nucl. Ener. Soc.*, 1976, vol. 15, pp. 253-56.
40. N. Prasad, G. Malakondaiah, and P. Rama Rao: *Scripta Metall.*, 1992, vol. 26, pp. 541-43.
41. N. Prasad, G. Malakondaiah, K. Muraleedharan, and P. Rama Rao: *J. Nucl. Mater.*, 1988, vol. 158, pp. 30-41.
42. C.E. Coleman: *J. Nucl. Mater.*, 1972, vol. 42, pp. 180-90.
43. B. Burton, A.T. Donaldson, and G.L. Reynolds: *Zirconium in the Nuclear Industry*, ASTM STP 681, ASTM, Philadelphia, PA, 1979, pp. 561-85.
44. G.E. Lucas and R.M.N. Pelloux: *Nucl. Technol.*, 1981, vol. 53, pp. 46-57.
45. G.E. Lucas and R.M.N. Pelloux: *Metall. Trans. A,* 1981, vol. 12A, pp. 1321-31.
46. G.E. Lucas, M. Surprenant, J. DiMarzo, and G.J. Brown: *J. Nucl. Mater.*, 1981, vol. 101, pp. 78-91.
47. P.J. Pankaskie: "Creep Properties of Zircaloy-2 for Design Application," HW-SA-2803, Hanford Atomic Products Operation, Richland, WA, 1962.
48. L.G. Bell: *Can. Metall. Q.*, 1963, vol. 2, pp. 119-42.
49. F. Tinti: *Nucl. Technol.*, 1983, vol. 60, pp. 104-13.
50. E.R. Gilbert and B. Mastel: *ANS Trans.*, 1969, vol. 12, pp. 132-33.
51. Y. Matsuo: *J. Nucl. Sci. Technol.*, 1987, vol. 24 (2), pp. 111-19.
52. F. Povolo and A.J. Marzocca: *J. Nucl. Mater.*, 1981, vol. 97, pp. 323-32.

53. A.T. Donaldson and R.C. Ecob: *Scripta Metall.*, 1985, vol. 19, pp. 1313-18.
54. C.C. Busby and K.B. Marsh: ''High Temperature Time-Dependent Deformation in Internally Pressurized Zircaloy-4 Tubing (LBWR Development Program),'' Bettis Atomic Power Laboratory Report No. WAPD-TM-1043, Westinghouse Electric Corporation, Pittsburgh, PA 1974.
55. C.C. Busby and L.S. White: ''Some High Temperature Mechanical Properties of Internally Pressurized Zircaloy-4 Tubing,'' Bettis Atomic Power Laboratory Report No. WAPD-TM-1243, Westinghouse Electric Corporation, Pittsburgh, PA 1976.
56. A.M. Garde, H.M. Chung, and T.F. Kassner: *Acta Metall.*, 1978, vol. 26, pp. 153-66.
57. A.M. Garde: *J. Nucl. Mater*, 1979, vol. 80, pp. 195-206.
58. H.M. Chung, A.M. Garde, and T.F. Kassner: ''Mechanical Properties of Zircaloy Containing Oxygen,'' Argonne National Laboratory Report No. ANL-76-121, Argonne National Laboratory, Argonne, IL, 1978.
59. G. Brun, J. Pelchat, J.C. Floze, and M. Galimberti: *Zirconium in the Nuclear Industry*, ASTM STP 939, ASTM, Philadelphia, PA, 1987, pp. 597-616.
60. M. Mayuzumi and T. Onchi: *J. Nucl. Mater.*, 1990, vol. 175, pp. 135-42.
61. M. Mayuzumi and T. Onchi: *J. Nucl. Mater.*, 1990, vol. 171, pp. 381-88.
62. K.L. Murty: *JOM*, 1999, vol. 51, pp. 32-39.
63. K.L. Murty, B.V. Tanikella, and J.C. Earthman: *Acta Metall. Mater*, 1994, vol. 42, pp. 3653-61.
64. K.L. Murty: *Trans. Ind. Inst. Met.*, 2000, vol. 53, pp. 107-20.
65. Y.-S. Kim: *J. Nucl. Mater.*, 1997, vol. 250, pp. 164-70.
66. J.H. Choe and J.H. Hong: *J. Kor. Inst. Met.*, 1984, vol. 22, pp. 613-20.
67. Y.-K. Park, T.-S. Kim, J.-H. Choi, and M.-Y. Wee: *J. Kor. Inst. Met. Mater.*, 2000, vol. 38, pp. 624-28.
68. H.E. Rosinger, P.C. Bera, and W.R. Clendening: ''The Steady State Creep of Zircaloy-4 Fuel Cladding from 940 to 1873 K,'' AECL-6193, Atomic Energy of Canada Limited, Whiteshell Nuclear Research Establishment, Pinawa, Manitoba, Canada, 1978.
69. G. Porsch, J. Fleisch, and B. Heits: *Nucl. Technol.*, 1986, vol. 74, pp. 287-98.
70. M. Peehs and J. Fleisch: *J. Nucl. Mater.*, 1986, vol. 137, pp. 190-202.
71. R.E. Einziger, H. Tsai, M.C. Billone, and B.A. Hilton: ''Examination of Spent Fuel Rods after 15 Years in Dry Storage,'' Report No. NUREG/CR-6831, ANL-03/17, Argonne National Laboratory, Argonne, IL, 2003.
72. R.E. Einziger, S.D. Atkin, D.E. Stellrecht, and V. Pasupathi: *Nucl. Technol.*, 1982, vol. 57, pp. 65-80.
73. R.E. Einziger and R. Kohli: *Nucl. Technol.*, 1984, vol. 67, pp. 107-23.
74. W. Goll, H. Spilker, and E. Toscano: *J. Nucl. Mater.*, 2001, vol. 289, pp. 247-53.
75. C. Pescatore and M.G. Cowgill: ''Temperature Limit Determination for the Inert Dry Storage of Spent Nuclear Fuel—Final Report,'' EPRI TR-103949, Brookhaven National Laboratory, Upton, NY, 1994.
76. P.J. Henningson, J.T. Willse, B. Cox, M.G. Bale, K.L. Murty, and W.A. Pavinich: ''Cladding Integrity under Long Term Disposal,'' Framatome Technologies Report No. 51-1267509-00, 1998.
77. R.L. Keusseyan, C.P. Hu, and C.Y. Li: *J. Nucl. Mater.*, 1979, vol. 80, pp. 390-92.
78. T.A. Hayes, R.S. Rosen, and M.E. Kassner: *J. Nucl. Mater.*, in press.